$D \approx (\delta r)^2/6\delta\tau$ using isotropic motion for simplicity. Then from eq 2 we obtain (with $\delta y \rightarrow \delta r$ for simplicity), $R_{\text{eff}} \approx 4\pi^2 D/P^2$. Now, for a nitroxide, the slow tumbling region is for $\tau_R \equiv (6R)^{-1} \gtrsim 10^{-8}$ s. But since we have $\langle D_\omega^2 \rangle \sim 0.1$ (cf. Table II), then in the present case we have $\tau_R \gtrsim 10^{-8}$ s^{-1}. Thus, motional averaging of the distortion effect would require $P^2/24\pi^2 D < 10^{-8}$ s. E.g., for $D \approx 10^{-8}$ (10^{-6}) cm^2/s, we would require a $P < 15$ (150) Å. A value of $P < 15$ Å seems very unlikely, since it is then of the order of the average dimension of a DPPC molecule, while $P < 150$ Å is not as unlikely but would require a rather fast D.

(35) R. F. Campbell, E. Meirovitch, and J. H. Freed, J. Phys. Chem., 83, 525 (1979).

ESR Studies of Low Water Content 1,2-Dipalmitoyl-*sn*-glycero-3-phosphocholine in Oriented Multilayers. 2. Evidence for Magnetic-Field-Induced Reorientation of the Polar Headgroups

Eva Meirovitch and Jack H. Freed*

Baker Laboratory of Chemistry, Cornell University, Ithaca, New York 14853 *(Received: May 6, 1980)*

In this continuation of ESR studies on a variety of spin probes incorporated into low-water-content 1,2-dipalmitoyl-*sn*-glycero-3-phosphocholine (DPPC) bilayers, results with the headgroup-region probes, PD-Tempone and VO^{2+}, are reported for the biaxial phase. The fluidity of the weakly ordered PD-Tempone probe is quite high for higher water content (14 wt %) but decreases for lower water content (9 wt %) (i.e., $R_\perp$, the diffusion coefficient, decreases from 10^9 to 10^8 s^{-1} and shows properties probably related to slowly relaxing local structure in the latter case). The VO^{2+} ions are, however, immobilized on the ESR time scale and weakly oriented. Both probes show distributions in local director, which, however, become better aligned as $\vec{H}$, the magnetic field, is tilted into the bilayer plane. Also both probes then have a preferential alignment perpendicular to the projection of $\vec{H}$ in this plane. These results are taken as definite evidence for cooperative headgroup alignment by the magnetic field. While positive (vs. negative) diamagnetic susceptibility is expected they could not be distinguished by these experiments. Anomalous results from a stearamide probe in the $L_\alpha(1)$ phase, viz. an unusually large observed splitting of 19.05 G with plate samples but typical splitting of 16.1 G with tube samples, is taken as evidence for significant differences in microscopic ordering properties of the DPPC samples resulting from different anchoring constraints imposed by the shapes of the holders. The nature of the biaxiality observed in the biaxial phase by other techniques is considered in the light of these ESR results.

I. Introduction

The addition of small amounts of water to dry phospholipids results in the formation of bilayer structures with a hydrophobic interior and two polar interfaces. In a preceding ESR spin-probe study (referred to in the following as 1)[1] we examined evidence for cooperative chain distortions taking place in the hydrophobic region of the bilayer; the subject of the present study is an examination of evidence for cooperative headgroup reorientation at the bilayer interface enhanced by external magnetic fields and by surface forces.

We studied 2–14 wt % water content DPPC both in the biaxial and in the $L_\alpha(1)$ phases, using the alignment technique of Powers and Pershan[2] to prepare uniform planar multilayers between parallel glass plates. In these aligned phases the main chain axes $\hat{d}_c$ of DPPC are perpendicular to the main headgroup axes $\hat{d}_h$ of the phospholipid molecules, and at low water content $\hat{d}_c$ is approximately parallel to $\hat{n}_m$, the normal to the plates and to the bilayers, implying that the $\hat{d}_h$ axes lie within the bilary plane, as illustrated in Figures 1 and 2.

Our ESR results on these phases show some distinctive and unusual characteristics for which we suggest interpretations relevant to an understanding of the physical properties of these phases. Thus we relate the phenomenon of magnetic-field-induced molecular reorientation, previously observed with model[3a] and biological[3b] membranes, to the molecular conformation of DPPC and to long-range cooperative alignment in the bilayer plane and between adjacent bilayers. We show that our results on the well-aligned DPPC samples are consistent with the hypothesis that, upon tilting the external field $\vec{H}$ away from $\hat{n}_m$, the DPPC headgroups reorient in the bilayer plane so as to optimize the angle between $\hat{d}_h$ and $\vec{H}$.

Surface-aligning forces are likely to contribute substantially to the long-range alignment of the headgroups. By replacing the parallel glass surfaces by a cylindrical sample holder, the boundary conditions are drastically altered. In support of this we find with a stearamide spin probe in the $L_\alpha(1)$ phase that by changing the sample geometry, not only the macroscopic alignment, but also the microscopic characteristics, as reflected in the ESR spectra of this probe, are substantially altered. Our findings with this probe (which is built of a stearic acid chain residue and a piperidine ring containing the nitroxide) are consistent with a hypothesis that in the plate samples the piperidine ring is intercalated between adjacent bilayers and with high ordering and probably experiences "very anisotropic" diffusion, whereas in tubes the familiar behavior[4] of low ordering and slightly anisotropic diffusion is encountered. Such a description would be consistent with a considerable decrease in the extent of lateral as well as interbilayer cooperativity in the latter case, while in the former the plates tend to layering which imposes rather severe conformational and dynamic restrictions on the stearamide molecule.

We do suggest that a cooperative in-plane "anchoring" of headgroups may be achieved in the plate samples during the growth process of the biaxial phase from the higher $L_\alpha(1)$ phase, inducing a nonzero biaxial birefringence. This

0022-3654/80/2084-3295$01.00/0

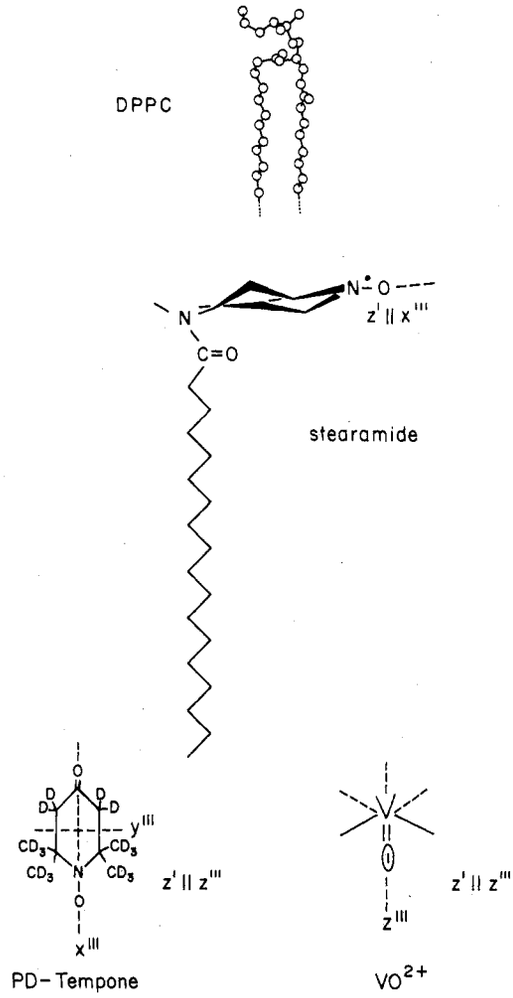

Figure 1. Schematic illustration of the various spin probe molecules and of the host DPPC molecule. x''', y''', and z''' are the principal axes of the magnetic tensors whereas z' denotes the principal axis of the ordering tensor.

interpretation of the optical biaxiality is in agreement with the light scattering,[2a] X-rays,[5] and ^{31}P NMR[6] results on DPPC bilayers.

Magnetic-field-induced reorientation of a liquid crystalline director has been observed with thermotropic smectic C phases[7,8] (where the director is tilted relative to the normal to the smectic layers), from which it was possible to estimate the elastic constant for reorientation of the smectic C director component (that is perpendicular to $\hat{n}_m$) about $\hat{n}_m$. The headgroup region of DPPC can be viewed as a special type of smectic C "phase" with a 90° tilt. Thus a systematic study as a function of magnetic field strength and orientation, as well as sample thickness, would enable one to estimate the analogous elastic constant for lyotropic liquid crystals. Our present results indicate that in lyotropic phases magnetic instabilities occur at similar external fields as in thermotropic phases for identical geometries.

Experimental details are summarized in section II, while the main results obtained with perdeuterated tempone (PD-Tempone) and VO^{2+} in the biaxial phase and with stearamide in the $L_\alpha(1)$ phase are presented and discussed in section III. (The structure of these molecules and of DPPC is shown in Figure 1.) In section IV we give further discussion in terms of other studies; our conclusions appear in section V.

II. Experimental Section

The details regarding sample preparation and recording

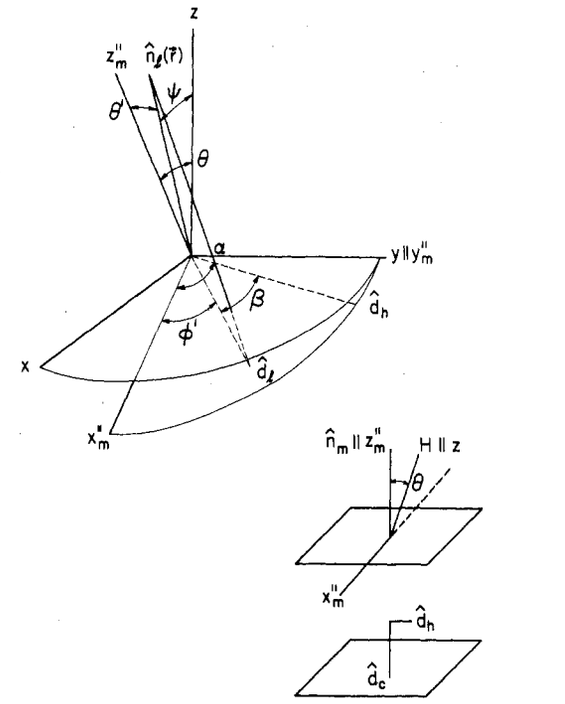

Figure 2. x_m'', y_m'', z_m'' represents the mean director frame of the structure with $z_m'' \| \hat{n}_m$ and x_m'' in the plane defined by $\hat{n}_m$ and $\vec{H}$. x_l'', y_l'', z_l'' is the local director frame with $\hat{n}_l(\vec{r}) \| z_l''$ and θ' and φ' denoting the polar and azimuthal angles of $\hat{n}_l(\vec{r})$ in the x_m'', y_m'', z_m'' frame, with $\hat{d}_l$ denoting the projection of $\hat{n}_l(r)$ in the x_m''–y_m'' plane. α is the angle between x_m'' and $\hat{d}_h$ and β between $\hat{d}_l$ and $\hat{d}_h$. x, y, z is the lab frame with $\vec{H} \| z$, θ denotes the angle between $\hat{n}_m$ and $\vec{H}$. ψ is the angle between $\hat{n}_l(\vec{r})$ and $\vec{H}$. We also define $x'y'z'$ to be the ordering frame of a particular probe molecule. d_c denotes the orientation of the undistorted chain and $\hat{d}_h$ the mean headgroup axis of a DPPC molecule, with $\hat{d}_h \perp d_c$.

of ESR spectra have been summarized in part 1.

Stearamide [(4-octadecanoyl)amino-2,2′,6,6′-tetramethylpiperidinyl-1-oxy] was purchased from Molecular Probes.

A stock solution of 0.1 M $VOSO_4$ obtained from Alfa Products in 3 N HCl at pH 1–2 was used; the final pH of the DPPC bilayers was estimated to be pH ≈ 3.0.

III. Results and Discussion

Although the relevant frames of reference have been defined in part 1, we shall summarize them for convenience in Figure 2. The x_m'', y_m'', z_m'' axes define the mean director frame of the multilayer sample with z_m'' parallel to $\hat{n}_m$, the bilayer normal, and x_m'' within the plane defined by z_m'' and $\vec{H}$; $z_l''(\vec{r})$, $y_l''(\vec{r})$, $z_l''(\vec{r})$ represent the local director frame with $\hat{n}_l(\vec{r})$ along z_l'' and θ' and φ' denoting the polar and azimuthal angles of z_l'' in the x_m'', y_m'', z_m'' frame. The x', y', z' axes represent the molecular ordering and diffusion axes of a particular probe, and x, y, z is the lab frame with $\vec{H} \| z$; θ is the angle between $\hat{n}_m$ and $\vec{H}$ and Ψ the angle between $\hat{n}_l(\vec{r})$ and $\vec{H}$ with $\cos\Psi = \cos\theta\cos\theta' - \sin\theta\sin\theta'\cos\varphi'$. The undistorted DPPC chain axes $\hat{d}_c$ are parallel to z_m'' and the main headgroup axes $\hat{d}_h$ lie within the x_m''–y_m'' plane.

A. PD-Tempone in the Biaxial Phase. The ESR spectra of PD-Tempone in the biaxial phase are poorly resolved for a water content below 14 wt %. We shall discuss in detail the results obtained for 14 wt % samples and then comment on lower water content structures in the light of these results.

The main features of the angular- (θ) dependent spectra illustrated in Figure 3a are characteristic of relatively high mobility, low ordering, and a substantial distribution of

TABLE I

	a_x'''	a_y'''	a_z'''	a_N	g_x'''	g_y'''	g_z'''	g_N
PD-Tempone in 14 wt % water content DPPC bilayers, biaxial phase	6.16	5.5	36.8	16.22	2.0088	2.0061	2.0027	2.00587
PD-Tempone in 9 wt % water content DPPC bilayers, biaxial phase	4.0	4.0	35.4	14.2	2.0088	2.0061	2.0027	2.00587
PD-Tempone in phase V (ref 13)	5.61	5.01	33.7	14.78	2.0088	2.0061	2.0027	2.00587
stearamide in the $L_\alpha(1)$ phase	7.26	5.23	36.1	16.1	2.0090	2.0061	2.0022	2.0058
1-acetylaminoperdeuterio-2,2',6,6'-tetramethylpiperidine in CD_3OD (ref 15b)	7.2	5.2	35.9	16.00	2.0090	2.0061	2.0022	2.0058
VO^{2+} in 2 wt % water content DPPC bilayers, biaxial phase	74.4	74.4	200.9	116.6	1.9785	1.9785	1.938	1.965
VO^{2+} complexed to trimethyl phosphate (ref 15a)	74.5	74.5	202.6	117.2	1.977	1.977	1.94	1.965

TABLE II

		$\langle D_{00}^2 \rangle$	λ	θ, deg	ρ	$10^{-8}R_\perp$, s^{-1}	N	$\hat{N}$	$\epsilon_s'/\epsilon_{ps}'$	T_2^{*-1}, G	temp, °C	E_{act}, kcal/mol
PD-Tempone in 14 wt % water content DPPC bilayers		+0.057	+0.41	90	0.0	10.0	2.0	1.0	1.0	0.3	26	
PD-Tempone[a] in 9 wt % water content DPPC bilayers						2.5				1.0	46	
						2.0				1.1	38	
		−0.052	−0.4	90	0.0	1.7	1.8	24.0	1.0	1.2	31	5.5
						1.4				1.3	26	
						1.5				0.4	46	
		+0.052	+0.4	0	0.0	1.1	1.0	1.0	30.0	0.5	38	6.6
						0.75				0.5	26	
stearamide[c] in 2 wt % water content DPPC bilayers	tube[b]	0.02	0.15		0.0	3.5	2.8	1.0	1.0	1.2	115	8.6
						1.5				1.3	90	
			−3.5		−0.09	0.3				1.2	115	
	plates	−0.305	−3.6	0	−0.07	0.17	39.0	10.0	1.0	1.3	103	11.2
			−3.6		−0.07	0.1				1.4	90	

[a] Negative ordering and $\theta = 0°$ is (in this dynamic range) indistinguishable from positive ordering and $\theta = 90°$. [b] The tube samples were simulated with $P(\Psi, \vartheta) = 1/4\pi$, with Ψ and φ denoting the polar and azimuthal angles of $\hat{n}_l(\vec{r}')$ in the xyz frame. [c] The observed hyperfine splitting for plates (tubes) was 19.07 G (16.3 G) at 90 °C and 18.8 G (16.2 G) at 115 °C.

$\hat{n}_l(\vec{r})$ relative to $\hat{n}_m$. As explained in part 1, the distribution of $\hat{n}_l(\vec{r})$ with respect to $\vec{H}$ reflected in the $\theta = 0°$ spectrum is identical with the distribution of $\hat{n}_l(\vec{r})$ relative to $\hat{n}_m$. To simulate the ESR line shape we proceeded as described in part 1 and find, similar to the hydrophobic probes in the $L_\alpha(1)$ phase (but unlike PD-Tempone in this phase), that a good fit between theory and experiment can only be obtained with a distribution function of the form

$$P(\theta',\varphi') = (\sin\theta')^{-1} \quad (1)$$

i.e., a two-dimensional (2D) spatial distribution as shown in Figure 3bI. Our calculations include homogeneous contributions to the line width of the individual components in the distribution as explained in part 1, based on a recent formulation of Moro and Freed,[9a] and the parameters used to simulate the spectra in Figure 3b are summarized in Tables I and II. The magnetic parameters were obtained by scaling the principal values of the hyperfine tensor of PD-Tempone in phase V by $a_{N(DPPC)}/a_{N(phase\ V)}$, with $a_{N(DPPC)}$ denoting the value of the hyperfine splitting in the isotropic phase occurring above $L_\alpha(1)$ (which was found to be nearly the same as a_N in $L_\alpha(1)$) and are given in Table I.

We interpret the disorder in $\hat{n}_l(\vec{r})$ relative to $\hat{n}_m$ for PD-Tempone in the biaxial phase in a manner similar to that we interpreted in I for the hydrophobic probes in the $L_\alpha(1)$ phase, i.e., in terms of cooperative chain distortions. Unlike our results with PD-Tempone in the $L_\alpha(1)$ phase, which indicated that the upper part of the DPPC chains close to the interface is essentially defect free (or else the PD-Tempone is diffusing relatively rapidly, cf. I) our results suggest that in the biaxial phase distortions occur over the entire chain length. This is consistent with neutron diffraction experiments on selectively deuterated uniform DPPC bilayers,[10] where one determines the distance x_0 of a particular deuterated segment from the center of the bilayer and ν, the $1/e$ half-width of the distribution in x_0. For 6 wt % water content, ν was found to be 1.5 Å for the C-4 segment of DPPC (with the carbonyl carbon being C-1) and 3.4 Å for C-15 in the $L_\alpha(1)$ phase while it is approximately 2.8 Å for all carbon atoms in the biaxial phase.[10a] These neutron diffraction results imply that the upper part of the chains are rather uniformly and highly ordered in the $L_\alpha(1)$ phase, while the flexibility of the chain increases gradually upon proceeding down the chain toward the end methyl group. In the biaxial phase, however, all the carbon atoms are substantially and equally "spread" about their mean position. Since the time scale of the diffraction experiment is related to very high frequencies ($\sim 10^{13}$ s^{-1}), what appears to be a static distribution in distances x_0 from such experiments may be either a static and/or dynamic disorder on the ESR time scale.

Note that our observed value for a_N of 16.2 G in the biaxial phase with 14 wt % water is very similar to that observed for PD-Tempone in pure water.[4] This indicates that PD-Tempone is located in the relatively polar region close to the bilayer interface at this water content.

For $\theta = 90°$ we first tried to simulate the experimental spectrum in Figure 3a with eq 1, similar to what had been done in part 1 for $\theta \neq 0°$. We found that the experimental spectrum *cannot* be simulated satisfactorily in this manner.

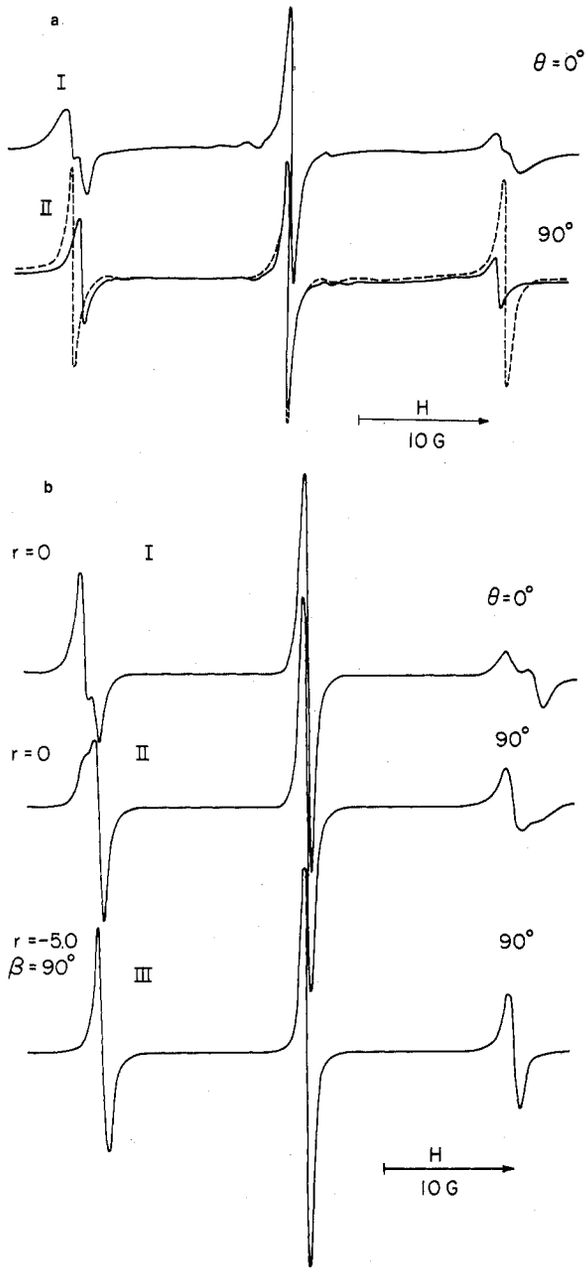

Figure 3. (a) ESR spectra of 10^{-3} M PD-Tempone dissolved in 14 wt % water content DPPC bilayers in a 150 ± 50 μm thick plate sample in the biaxial phase at room temperature for field orientations as denoted in the figure; the dashed line represents the ESR spectrum of 10^{-3} M PD-Tempone in D_2O at pH ≈6.00 and was included to show that we do encounter here a single-species spectrum with no bulk species present. (b) I. Calculated spectrum for $\theta = 0°$ obtained by using the formulation of Moro and Freed[10a] with the distribution function $P(\theta',\varphi') = (\sin\theta')^{-1}$ and the parameters given in Tables I and II. II. Same as I for $\theta = 90°$. III. Same as II with $P(\theta',\varphi') = e^{r\sin^2\theta\sin^2(\varphi'+\beta)}(\sin\theta')^{-1}$ with $r = -5.0$ (5.0) and $\beta = 90°$ (0°).

The calculated spectrum displays particular powderlike features reflecting a considerable distribution of $\hat{n}_l(\vec{r})$ axes relative to $\vec{H}$, whereas the experimental spectrum consists of a well-defined triplet suggestive of a unique orientation of $\hat{n}_l(\vec{r})$ relative to $\vec{H}$, as illustrated in parts bII and aII of Figure 3. Also, the $\theta = 90°$ spectra are unchanged when $\vec{H}$ is rotated in the x_m''–y_m'' plane. We considered next the possibility of a magnetic-field-dependent angular distribution function. Since the ESR spectra of the hydrophobic probes discussed in detail in part 1 could be simulated in both the $L_\alpha(1)$ and in the biaxial phase simply with eq 1, any such collective reorientation of local directors that is sensed by PD-Tempone is probably related to the headgroup region only. (Note that the hydrophobic probes were only studied in the easier to prepare 2 wt % samples.)

Magnetic-field-induced reorientation in phospholipid membranes has been observed previously with ESR spin probes.[3] Gaffney and McConnell[3] have interpreted the ESR line shape of spin-probe-doped egg lecithin assuming that the lyotropic liquid crystal is a smectic C-type phase with the main chain axes tilted at about 30° relative to the smectic layer normal and, similar to observations on thermotropic smectic C phases,[7] the director reorients freely about the normal to the smectic layer so as to minimize the magnetic free energy, F_{mag}, i.e., the angle between the director and $\vec{H}$ ($F_{mag} = -\vec{\mu}\cdot\vec{H} = \Delta\chi_d H^2\cos^2\psi$, with μ denoting the magnetic moment and $\Delta\chi_d$ the anisotropy in the bulk magnetic susceptibility). In our case the tilt of the main chain axes $\hat{d}_c$ relative to $\hat{n}_m$ is only 10–15° for 14 wt % water and even smaller for lower water content;[1,5] such a small tilt and the smectic C model cannot explain our PD-Tempone spectra in the biaxial phase. On the other hand, the main headgroup axis $\hat{d}_h$ is tilted at about 90° relative to $\hat{n}_m$.[7,10c] Thus, assuming that the headgroup region behaves as a smectic C liquid crystal with $\hat{d}_h$ being the "smectic director", we expect, for high fields and thick samples,[7,8] that, upon tilting $\vec{H}$ away from being parallel to $\hat{n}_m$, all $\hat{d}_h$ axes reorient in the bilayer plane so as to optimize the angle between $\hat{d}_h$ and $\vec{H}$. For $\theta = 90°$, all $\hat{d}_h$ axes will then tend to be fully aligned relative to $\vec{H}$.

We can analyze the spectral effects of such a cooperative headgroup reorientation in the magnetic field by considering a simple model. We first assume that $\hat{d}_h(\vec{r})$ remains in the x_m''–y_m'' plane at an angle α with x_m'' as shown in Figure 2. So if the PD-Tempone, located in the headgroup region, is indeed sensitive to reorientation of $\hat{d}_h(\vec{r})$ by the magnetic field, then its ESR spectrum should show a dependence upon the angle γ between $\vec{H}$ and $\hat{d}_h(\vec{r})$. From Figure 2 we have $\cos\gamma = -\sin\theta\cos\alpha$, so that $F_{mag} = \Delta_{\chi d}H^2\cdot\sin^2\theta\cos^2\alpha$.

Now the exact manner in which the PD-Tempone is affected by magnetic effects is not yet clear. Suppose we assume a definite correlation between $\hat{d}_h(\vec{r})$ and the projection of $\hat{n}_l(\vec{r})$ in the x_m''–y_m'' plane (call it $\hat{d}_l(\vec{r})$) such that $\alpha = \varphi' + \beta$, with PD-Tempone sensing $\hat{n}_l(\vec{r})$ directly. This suggests we try a distribution function of form

$$P(\theta',\varphi') \propto e^{r\sin^2\theta\cos^2(\varphi'+\beta)}(\sin\theta')^{-1} \qquad (2)$$

Equation 2 reverts to eq 1 for $\theta = 0°$. We find that for the two limiting cases of $\beta = 0$ and 90° we can successfully fit the $\theta = 90°$ spectrum in Figure 3 provided we use $r \approx -5.0$ or +5.0, respectively. Thus, in the case of $\beta = 0°$ we would preferentially have $\hat{d}_l \parallel \hat{d}_h$ and $\hat{d}_h \perp x_m''$ (or negative diamagnetic anisotropy), while for $\beta = 90°$, $\hat{d}_l \perp \hat{d}_h$ and $\hat{d}_h \parallel x_m''$ (or positive diamagnetic anisotropy). While we cannot distinguish between positive vs. negative diamagnetic anisotropy from this experiment alone, it still follows that $\hat{d}_l$ will preferentially align parallel to y_m'', i.e., perpendicular to the projection of $\vec{H}$ in the x_m''–y_m'' plane. On the basis of simple models we would prefer $\hat{d}_l \perp \hat{d}_h$ so $\beta = 90°$ and there is positive diamagnetic anisotropy.

If, however, we assume no correlation between α and φ', then a model in which PD-Tempone was sensitive to $\hat{d}_h$ could be the simple limit where its "local director" is a composite with polar angle θ' (from $\hat{n}_l(\vec{r})$) and azimuthal angle α, or $\alpha + \pi/2$. We now use $\hat{d}_l$ as the component of the composite director in the x_m''–y_m'' plane; thus use of α implies $\hat{d}_l \parallel \hat{d}_h$, while use of $\alpha + \pi/2$ implies $\hat{d}_l \perp \hat{d}_h$. Then a similar analysis leads to similar conclusions, viz. $\hat{d}_l$ prefers to align along y_m'' for $\theta \neq 0°$, but one does not

know from this result alone whether the headgroup exhibits positive or negative diamagnetic susceptibility.

The first case involving correlation between $\hat{d}_l$ and $\hat{d}_h$ seems somewhat more reasonable to us. At any rate, defects in the main chain region should not be affected by the headgroup reorientation in order to be consistent with our results using the hydrophobic probes albeit at lower water content (2 wt %). In support of this, it was shown with ^{31}P NMR[11,12] that the onset of dynamic headgroup reorientation occurred while the chains remained immobilized. (Actually our model could allow for the chains themselves to reorient while the local director representing a cooperative distortion wave does not.)

A comment is appropriate at this point about the sensitivity of our ESR results to the precise choice of distribution function such as eq 2. Thus we tried a variation on eq 2 such that $\sin^2\theta\cos^2\varphi'$ is replaced by $\sin^2\theta\sin^2\theta'\cos^2\varphi'$ and we found that the $\theta = 90°$ spectrum could again be satisfactorily fit for $r \approx -5.0$. Thus, while the ESR results cannot distinguish between forms similar to eq 2, the successful variants on this form are still consistent with (1) a substantial magnetic-field-induced reorientation in the headgroup region and (2) a preferential alignment of $\hat{d}_l$, the smectic C-type director (sensed by the PD-Tempone), along y_m'' in the x_m'–y_m'' plane, i.e., perpendicular to the projection of $\vec{H}$ in this plane. Clearly eq 2 is the simplest statement of these matters.

Further evidence for this magnetic-field-induced headgroup reorientation comes from an analysis of VO^{2+} spectra. However, before we consider these spectra we wish to say a few words about the PD-Tempone results with lower water content.

DPPC with Lower Weight Percent Water. The ESR spectra obtained by using PD-Tempone probe in 9 wt % water are similar to those of the 14 wt % content samples, although spectral resolution is considerably lower. This is found to be due to a decreased rate of rotational reorientation (cf. Table II). Also, there is increased ordering of $\hat{n}_l(\vec{r})$ so that eq 1 had to be modified to $P(\theta') \propto e^{-4.5\sin^2\theta'}(\sin\theta')^{-1}$ for $\theta = 0°$. Also the hyperfine tensor required readjustment to a lower a_N. We suspect these features imply either some increased intermolecular interactions experienced by the PD-Tempone at the DPPC headgroup at lower water content in the biaxial phase and/or some relocation of the probe a little further from the headgroup region (cf. below). Again the spectra for $\theta = 90°$ could be fit only when the above distribution for $P(\theta')$ was multiplied by the factor $e^{-3.5\sin^2\theta\cos^2(\varphi'+\beta)}$. From a complete line-shape analysis (cf. part 1) it was possible to fit the spectrum including motional effects, and the results appear in Table II. These results show that, unlike the 14 wt % case, a simple rotational model does not fit the spectra. Instead, one must invoke a model of very anisotropic viscosity or, alternatively, a fluctuating torque model[13] with very slow fluctuations from the surroundings (i.e., $\epsilon \gg 1$). Alternatively, one may invoke a model of slowly relaxing local structure.[9b] These results and the spectral observations requiring them (i.e., unusually large widths of the two outer hyperfine lines) were characteristic of previous observations with this probe in nematic[13] and smectic[9b] phases. The results of Lin and Freed[9b] on PD-Tempone are consistent with the probe being gradually expelled from the more-ordered regions to the less-ordered hydrocarbon chains as the liquid-crystalline phases become more ordered (due to reduction of temperature). It may be that at least some of our observations of PD-Tempone in the biaxial phase of DPPC reflect a similar trend as the water content is reduced from 14 wt %. The 2 wt % water samples containing PD-Tempone were too broad for any extensive analysis, but the a_N was estimated to be similar to that for the 9% samples, and the line shapes appear to have the distinctive features characteristic of a $(\sin\theta')^{-1}$ distribution or modification we found for 9 wt % water.

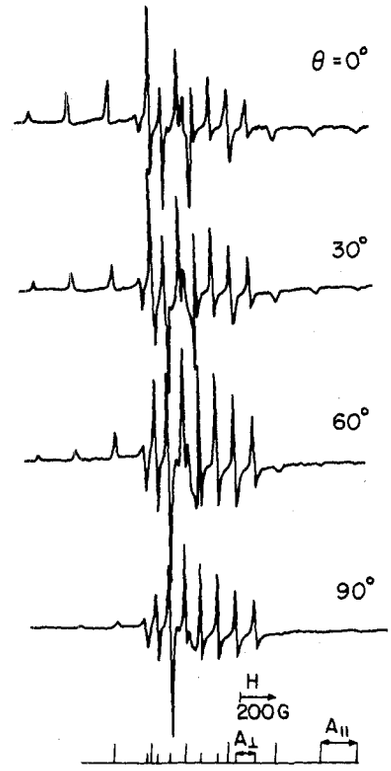

Figure 4. Experimental ESR spectra of 10^{-3} M $VOSO_4$ dissolved in 2 wt % water content DPPC bilayers in a 150 ± 50 μm thick plate sample in the biaxial phase at room temperature for field orientations as denoted in the figure.

B. VO^{2+} in the Biaxial Phase. The experimental spectra obtained for VO^{2+} in the (2% water) biaxial phase at room temperature for various orientations θ are shown in Figure 4. The invariance of the spectra upon lowering the temperature to −150 °C indicates that these are *rigid* limit spectra corresponding to a $S = {}^1/_2$ and $I = {}^7/_2$ axially symmetric VO^{2+} radical, including 16 peaks from 8 parallel ($\psi = 0°$) and 8 perpendicular ($\psi = 90°$) lines. From the positions of these peaks we obtained the principal values of the **A** and **g** tensors listed in Table I, and using these values we have calculated a three-dimensional (3D) isotropic powder spectrum with $P(\theta',\varphi') = 1/4\pi$ illustrated in Figure 5b. By comparing the 3D calculated powder spectrum with the experimental trace for $\theta = 0°$ in Figure 4a we notice that in the experimental spectrum the parallel peaks are too intense and too asymmetric as compared to the theoretical lines. We have recalculated the powder spectrum with $P(\theta',\varphi') = e^{-\lambda\sin^2\theta'}$, thus allowing for a nonzero ordering (with $z' \parallel z''$) relative to $\hat{n}_m$, and with $\lambda = 0.56$ we obtained spectrum a in Figure 5 which we consider to be a good fit to the experimental $\theta = 0°$ spectrum in Figure 4. This result corresponds to a low microscopic ordering of the VO^{2+} probe and is discussed further below.

We next calculated spectra for $\theta = 0$, 30, 60, and 90° with the same $P(\theta',\varphi')$, and we obtained the traces shown in Figure 6. By examining Figure 4 we notice that the main change in the experimental spectra upon going from $\theta = 0°$ to $\theta = 90°$ is a substantial decrease in the relative intensity of the parallel vs. the perpendicular peaks until, for $\theta = 90°$, an approximately one-site spectrum, corresponding to the perpendicular orientation, is obtained. This feature is *not* reproduced adequately by the theo-

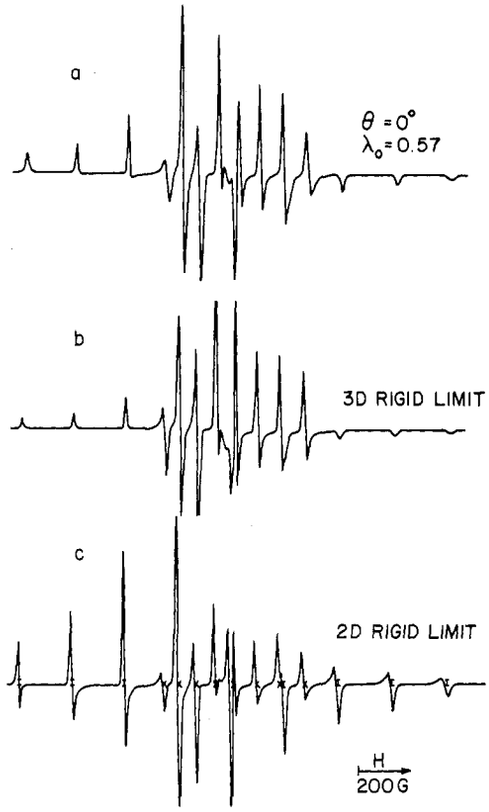

Figure 5. Calculated rigid-limit spectra for a $S = {}^1/_2$ and $I = {}^7/_2$ radical with $a_{x'''} = a_{y'''} = 74.4$ G, $a_{z'''} = 200.9$ G, $g_{x'''} = g_{y'''} = 1.9785$, and $g_{z'''} = 1.938$ and m_I dependent intrinsic line widths T_2^{*-1} ranging between 5.0 and 12.0 G, determined by means of a best-fit procedure. Spectrum a was calculated with $P(\theta',\varphi') = e^{-0.57\sin^2\theta'}$, spectrum b with $P(\theta',\varphi') = 1/4\pi$ and spectrum c with $P(\theta',\varphi') = (\sin\theta')^{-1}$. The x symbols denote the position of the $z''' \parallel H$ resonances and the I symbols the $z''' \perp H$ resonances.

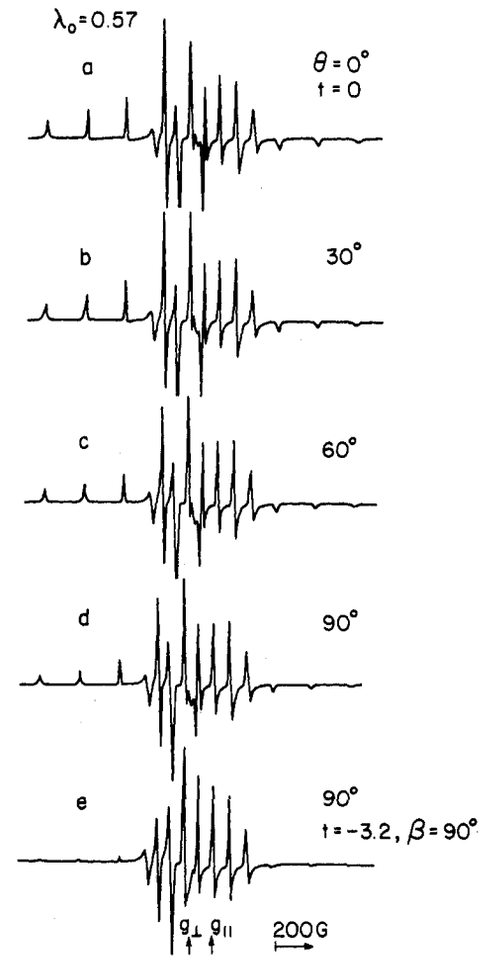

Figure 6. (a) Same as spectrum 5a; (b–d) same as a for $\theta = 30$, 60, and 90°, respectively; spectrum e was obtained for $\theta = 90°$ and $P(\theta',\varphi') = e^{\lambda_0[1+t\sin^2\theta\cos^2(\varphi'+\beta)]\sin^2\theta'}$ with $\lambda_0 = -0.57$, $t = -3.2$ (3.2), and $\beta = 90°$ (0°).

retical spectra a–d in Figure 6, the main discrepancy occurring for $\theta = 90°$ (compare the bottom trace Figure 4 with spectrum d in Figure 6). Basically, the effect is similar to the one observed with PD-Tempone; the distribution of z' axes in the theoretical spectra is greater than in the experimental ones. Therefore, we then tried the modified form $P(\theta',\varphi') \propto e^{-0.56\sin^2\theta'+r\sin^2\theta\cos^2(\varphi'+\beta)}$ as suggested by eq 2, and now θ' and φ' are the polar and azimuthal angles of z' of VO^{2+} in the x_m'', y_m'', z_m'' frame but again $\alpha = \varphi' + \beta$ with β a fixed phase relation. We find, however, that for $\theta = 90°$ this is still *not* a satisfactory form. Note that this form implies that the magnetic-free-energy term related to headgroup-induced reorientation may simply be added to the weak ordering term for vanadyl. The ordering of the vanadyl is an *indirect* probe of the headgroup alignment, the $\lambda = 0.56$ result from the rigid-limit spectra being a composite of (weak) ordering of the VO^{2+} relative to the headgroups and any mosaicity in alignment of the headgroups (see below). [This is somewhat different from the PD-Tempone case for which the rapid motion relative to its local director just required that the macroscopic distribution of local directors be included in describing any powderlike features of the ESR spectrum.] We can better represent the composite effects on VO^{2+} by utilizing

$$P(\theta',\alpha) \propto e^{-\lambda\sin^2\theta'} \tag{3a}$$

with

$$\lambda = \lambda(\theta,\alpha) = \lambda_0[1 + t\sin^2\theta\cos^2(\varphi' + \beta)] \tag{3b}$$

(where for simplicity we shall let $\beta = 0$ or 90°). That is, the (dimensionless) ordering potential λ for VO^{2+} is a function of the degree of alignment of the headgroups in the magnetic field, which, as we have seen, has the angular factor $\sin^2\theta\cos^2\alpha$. From the above discussion we take $\lambda_0 = 0.56$. We obtained, with the values $\beta = 0°$ and $t = 3.2$ (or $\beta = 90°$ and $t = -3.2$) spectrum e in Figure 6 for $\theta = 90°$, which is a very good fit to the $\theta = 90°$ experimental spectrum in Figure 4. This result is very similar to the implications of the PD-Tempone study. Thus, while the z' axis for VO^{2+} prefers to align parallel to z_m'' for $\theta = 0°$, when $\theta \neq 0°$ there is an additional preferential alignment such that for $\theta' > 0°$ the projection of z' in the x_m''–y_m'' plane prefers to align along y_m'' (i.e., perpendicular to the projection of $\vec{H}$ in this plane).

We note also that the spectra for $\theta = 90°$ are invariant to reorienting $\vec{H}$ in the x_m''–y_m'' plane as we would expect.

A similar conformation of the vanadyl in liquid crystalline micelles (i.e., z''' perpendicular to the bilayer plane) was suggested previously by Campbell and Hanna.[14] Their results imply that the VO^{2+} ion is bound at the interface in the lyotropic system they studied (sodium octanoate/octanoic acid/water) by complexation to carboxylic groups of the solvent molecules. Furthermore, the similarity in the magnitude of the rigid-limit magnetic parameters (**A** and **g** tensor) of VO^{2+} in these systems to those of vanadyl acetate are considered to strongly support the hypothesis of the vanadyl ions being bound at the bilayer interface. We find that our rigid-limit values are very similar to the vanadyl–trimethyl phosphate complex[15a] (see Table I), indicating that the VO^{2+} ion is likely to be bound to the PO_4^- group of the DPPC molecule.

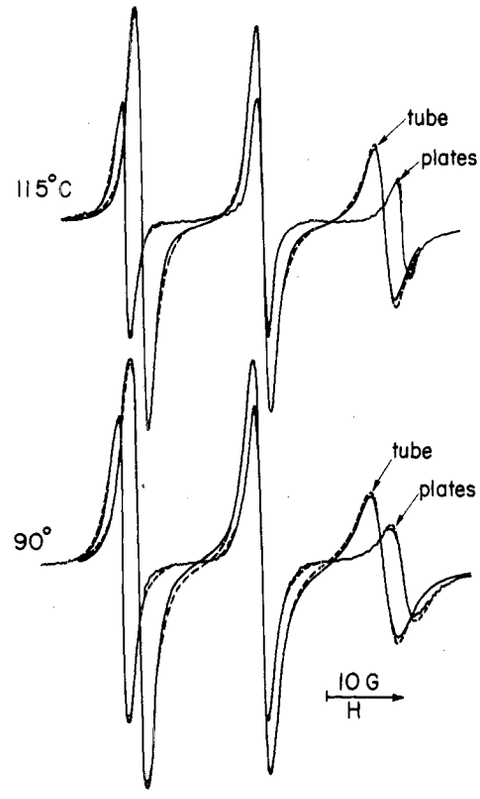

Figure 7. Experimental ESR spectra of 10^{-3} M stearamide in 2 wt % water content tube and plate samples in the $L_\alpha(1)$ phase at various temperatures (—); the plates were 150 ± 50 μm thick and the external field H was perpendicular to the plates. Corresponding calculated spectra with the parameters given in Tables I and II, with $P(\psi,\varphi) = 1/4\pi$ for the tube samples and $\theta = 0°$ for the plates (---).

Unlike PD-Tempone in the biaxial phase, VO^{2+} does not reflect the chain distortions, in agreement with VO^{2+} binding on top of the polar interface. To illustrate this point we have calculated spectrum c in Figure 5 which would correspond to a 2D distribution. It is seen to be significantly different from the experimental spectrum in Figure 4 obtained for $\theta = 0°$.

We now consider further the distribution function eq 3 for $\theta = 0°$ in terms of the combined effects of very low ordering and headgroup mosaicity. Neutron diffraction experiments[9b] have shown that $\nu = 3$ Å for deuterated segments in the headgroup, which is larger than the ν values for the chain segments.[9a] The extent of out-of-plane deviations of the $\hat{d}_h$ axes has been estimated by ^{31}P NMR[6] to be approximately ±15%; furthermore, a higher degree of headgroup mosaicity would be inconsistent with our results for the biaxial phase presented in part 1, if we have $\hat{d}_h \perp \hat{d}_c$. We thus conclude that low ordering of VO^{2+} relative to $\hat{d}_h$ is the main reason for the small value of λ_0 that we have found.

Our result that the VO^{2+} ordering is significantly improved as the headgroups are aligned by the magnetic field seems to imply that VO^{2+} can better intercalate between the headgroups of adjacent bilayers once they have aligned, i.e., there must be some cooperativity between the bilayers in this process.

C. Stearamide in the $L_\alpha(1)$ Phase. The long and flexible stearamide probe, usually associated with the headgroup region, exhibits very particular characteristics when dissolved in 2 wt % water content DPPC bilayers. Spectra obtained with cylindrical tube and plate samples in the $L_\alpha(1)$ phase are presented in Figure 7. For both types of sample geometries, the spectra are *independent* of orientation, but otherwise they are considerably different. The most prominent difference is that the observed splitting is 19.05 G at 95 °C for the plates, which is considerably higher than the common range of values for the hyperfine splitting for piperidine derivatives (14.5–16.5 G)[5] and approximately 16.2 G for the cylindrical tube samples. This is to be compared with the value of 16.1 G measured in the isotropic phase, and we scaled the **A** tensor (cf. section A) by comparison to 4-acetylaminoperdeuterio-2,2′,6,6′-tetramethylpiperidinyl-1-oxy in CD_3OD[15b] (see Table I), since its a_N and structure are similar.

In the macroscopically disordered tube sample (cf. part 1), there is little microscopic ordering which only shows up from a detailed line-shape analysis. Thus with a complete line-shape simulation we found that throughout this phase the stearamide probe experiences weak and nearly temperature-independent axially symmetric ordering with $\lambda = 0.15$, anisotropic diffusion with $N = 2.8$, and a decrease in the molecular reorientation rate from $R_\perp = 3.5 \times 10^8$ s^{-1} at 115 °C to $R_\perp = 1.5 \times 10^8$ s^{-1} at 90 °C. We estimate an activation energy of about 8.6 kcal/mol (see Table II). These results are in reasonable agreement with previous studies of stearamide in phospholipid bilayers,[4] showing that the piperidine ring is weakly ordered due to extensive flexibility of this probe.

The results for the plate sample are very surprising. It appears at first sight difficult to rationalize such a large change in observed splitting by just a change in the geometry of the sample holder, since it appears that this change must have brought about a change in microscopic properties of the probe. We do not believe that a change in the holder could have any substantial effect on the value of a_N, especially since a value of $\langle a \rangle = 19.05$ G is much greater than what has been obtained before.[4] On the other hand, if it were now highly ordered in the well-aligned $L_\alpha(1)$ phase, then we could estimate the value of $\langle a \rangle \approx {}^1/_2(a_{y'''} + a_{z'''}) = 20.7$ G for the limit of complete negative ordering with $x''' \parallel z'$. We have performed detailed line-shape simulations yielding $\lambda \approx -3.6$ and $\rho \approx -0.08$. However, good fits could only be obtained with very high values of asymmetry in both the rotational diffusion tensor and the microviscosity tensor (cf. Table II). While these results are particular to the models used in the analysis, they do suggest unusual properties. First, we do note that the high negative ordering would be consistent with the piperidine ring being intercalated in the headgroup interface region between adjacent bilayers. It is, however, difficult to conceive of the entire stearamide molecule being intercalated in this interface in view of the hydrophobic nature of the long stearic-acid chain. Instead, we conceive of the hydrophobic chain on the average parallel to the DPPC chains. Thus the stearamide could take on an ordered conformation similar to the DPPC molecules, viz., a chain aligned along $\hat{n}_m$ and a headgroup aligned perpendicular to $\hat{n}_m$. For such an ordered conformation, one would indeed expect a dynamic mode for the probe consisting in a "very anisotropic" internal reorientation[16] of the piperidine segment which is effectively decoupled from the reorientation of the highly ordered chain.

We have built a space-filling model to examine this conformational aspect and, in particular, to try and relate the main diffusion axis of the piperidine ring to the molecular conformation. We found that the segmental motion of the nitroxide moiety should neither take place about the CH–NH nor about the CO–NH chemical bonds (see Figure 2). Rather, there would be a mean symmetry axis, similar to the results obtained by Campbell et al.[12] for the internal reorientation of the DPPC headgroup studied by ^{31}P NMR. Furthermore, we found that the upper (i.e.,

close to the polar interface) part of the stearic acid chain residue would have to be distorted from an all-trans conformation parallel to $\hat{n}_m$ should $x''' \perp \hat{d}_c$(DPPC), while the main chain axis of stearamide is parallel to $\hat{d}_c$(DPPC). [This situation might arise since the stearic acid residue is longer than the palmiatic acid residues of the DPPC molecules and the long stearic chain is likely to be bent close to the polar interface, subject to the constraints imposed by the hydrophobic nature of the chain and the location of the piperidine ring.]

This model would then imply that the effect of sample geometry on the microscopic characteristics is due to the presence in the case of well-aligned samples (and the absence for unaligned samples) of large arrays of uniform bilayers with strong cooperative interbilayer forces prevailing in the headgroup regions. Further, the particular structure and conformation of stearamide with polar headgroup and hydrophobic chain must satisfy very distinctive requirements for packing into the ordered arrays. On the other hand, the homologue of stearamide, tempamine, with a single hydrogen replacing the stearic acid residue, was found in part 1 to exhibit the same microscopic behavior in both tube and plate samples (i.e., weak x''' ordering). It is of interest to note that Powers and Pershan[2b,c] found with oriented low water content DPPC containing chlorophyll a that the porphyrin ring is also restricted to the bilayer interface.

There still remains the feature of the invariance of the plate spectrum to all reorientations of $\vec{H}$ relative to x_m'', y_m'', z_m'' and whether the model suggested above is at all consistent with it. Thus, we recall from part 1 that the weakly ordered headgroup probes, Tempone, Tempamine, etc., showed smectic A-type spectra in the $L_\alpha(1)$ with the usual spectral variations as a function of θ. The only way we can rationalize this spectral invariance is to assume the following: (1) In the $L_\alpha(1)$ phase (just as in the biaxial phase) the headgroup axes $\hat{d}_h$ reorient within the bilayer plane so as to optimize the angle with $\vec{H}$ and, because of the greater fluidity of this phase this process is essentially complete for $\theta > 0°$, we have $\hat{d}_h \parallel x_m''$ or $\hat{d}_h \parallel y_m''$ corresponding to positive or negative diamagnetic anisotropy (cf. sections A and B). (2) The x''' axis, which is approximately the main symmetry axis of the piperidine ring, tends to lie perpendicular (parallel) to $\hat{d}_h$ for positive (negative) diamagnetic anisotropy (cf. sections A and B). Then for $\theta \neq 0°$ we have $x''' \perp \vec{H}$ essentially independent of θ as we required.

We regard the above model to be an interesting but speculative one, which we suggest in our attempt to explain the very unusual experimental observation of the large differences between plate vs. tube samples for the stearamide probe. The model seems to us not inconsistent with our other results and those of other studies, but further studies are required before one can have confidence in it.

IV. On the Nature of the Biaxiality in DPPC Bilayers at Low Hydration

Powers and Pershan[2b,c] have suggested that the biaxiality detected in low water content bilayers is mainly due to the headgroup region, based on changes in the uniaxial and biaxial birefringence (and other properties) or pure DPPC–water mixtures upon incorporating into the bilayers various components. Thus, species associated with the headgroup region, e.g., Na^+ and Ca^{2+} ions, chlorophyll a, etc., mainly affected the biaxial birefringence, whereas gramicidin A, associated with the chain region, mainly affected the uniaxial birefringence. Light scattering by undulations in the monohydrate DPPC bilayers has been observed by Powers and Clark[2a] in the $L_\alpha(1)$ phase. These undulations are described by the parameters $C \lesssim 10^{-5}B$ and $\lambda = (K/B)^{1/2} \sim 100A$, where B is the elastic constant associated with compression of the layers, K is the second-order elastic constant associated with bending of the individual layers, and C is the (shear) elastic constant associated with sliding layers over one another (smectic phases with no coupling between layers have $C = 0$). The authors state that upon entering the biaxial phase the scattering abruptly disappears indicating that (below the phase transition) $C \sim B$, i.e., a substantial coupling between adjacent layers and therefore some sort of three-dimensional crystalline ordering develops within the biaxial phase.[4]

^{31}P NMR measurements[6] on 2 wt % water content DPPC bilayers were shown to explicitly imply "anchoring" of headgroups in a preferred orientation within the bilayer plane (i.e., the x_m''–y_m'' plane), although the structures were found to be highly mosaic.

Recent crystallographic measurements[5] imply that upon lowering the temperature of a monohydrate sample to the biaxial phase strong long-range correlative interactions operate both between adjacent molecules within the same layer and between neighboring layers. On the other hand, with higher water content, the X-ray results suggest a decrease in the local cooperativity.

Thus, for the low water content DPPC there is evidence for (a) a preferential alignment or "anchoring" of the headgroup in the bilayer plane as well as (b) interbilayer correlations in this headgroup "anchoring" such that a *macroscopic* biaxial birefringence is observed. Our ESR results suggest that this "anchoring" is weak enough that the headgroups may readily be realigned with considerably improved alignment by magnetic fields of 3.3 kG both in the biaxial and in the $L_\alpha(1)$ phases when the field has a substantial component in the x_m''–y_m'' plane. When there is no aligning component, our results are consistent with considerable mosaicity in the headgroup. Also, our results lead us to suspect that the anchoring by the plates plays an important role in establishing the long-range cooperativity leading to the overall biaxiality. That is, plate anchoring establishes a preferential headgroup alignment which is then transmitted by interbilayer cooperativity (associated with a nonnegligible value for C). Thus the birefringence observed is what Born and Wolf[17] refer to as a "form birefringence", i.e., an overall biaxiality arising mainly from anisotropy on a scale much larger than molecular, related to a repeating entity with a symmetry lower than uniaxial rather than being due to anisotropic properties of molecules. In this case the biaxiality is directly related to the morphology of the structure, i.e., the extent of headgroup "anchoring".

In a recent study of thermal and strain-induced defects in the $L_\alpha(1)$ phase of low water content DPPC bilayers it is pointed out that, in certain cases, there is a nonzero biaxial birefringence in this phase, due to the curvature of the smectic bilayers in the form of parabolic focal conics.[18] Apparent biaxiality, due to oriented defects in samples of lamellar liquid crystals, has been also reported recently.[19] These are examples of another type of "form" biaxiality. This situation is similar to the different morphologies observed with thermotropic smectic C liquid crystals,[7,8a,20] where external factors such as the shape of the sample holder and the orientation of the magnetic field were found to influence molecular orientations. It might be that the high resistance to compression within the bilayer plane, which is particular to the biaxial phase and is implied by Brillouin scattering experiments,[2c] is also related to cooperative headgroup anchoring resulting in

a suppression of long-wave density fluctuations.

Griffin et al.[16] mention unsuccessful attempts to use an external magnetic field to align DPPC bilayers. However, throughout these attempts, the magnetic field was turned on only after the biaxial phase was obtained[21] by the method outlined in ref 2 in the absence of an external field. Assuming that the process of "growing" the biaxial phase is similar to a regular crystal growth mechanism, one can visualize the cooperative headgroup anchoring occurring in very much the same way as the orientation-dependent growth of a single crystal, determined by the experimental conditions. In this case a magnetic field applied in the x_m''–y_m'' plane *during* the growth process might assist in improving headgroup alignment. (Similar techniques have been used to align thermotropic liquid crystals.[20]) Such an experiment has not been yet performed.

Finally, we note that the microscopic nature of the interbilayer cooperativity yielding cooperative anchoring is not known yet. One possible mechanism would arise from a cooperativity between headgroup alignment and chain defect something like a model we have already discussed. However, our results in this work and in part 1 do not show any such cooperativity involving the lower chain region at least for 2 wt % water samples. Another possibility would be some cooperativity between headgroup orientation in the x_m''–y_m'' plane and preferential alignment in this plane of the two DPPC chains which might not be inconsistent with our results.

V. Conclusions

(1) In the low water-content biaxial phase of DPPC, headgroup probes such as PD-Tempone and VO^{2+} exhibit spectra as a function of tilt angle θ of the magnetic field $\vec{H}$ relative to the bilayer normal $\hat{n}_m''$, which can only be satisfactorily explained by a distribution function for the local directors (sensed by the probes) that depends upon the angle between $\vec{H}$ and the projection of the local director in the bilayer (x_m''–y_m'') plane.

(2) These observations are taken as definite evidence for the DPPC headgroups being oriented by the magnetic field when $\theta \neq 0°$, while the local directors representing distortions in the main part of the DPPC chains are essentially unaffected by the magnetic field for 2 wt % water content samples (cf. part 1).

(3) In the case of a stearamide probe in the $L_\alpha(1)$ phase, it was shown that the microscopic properties of the probe are altered by changing the nature of the macroscopic boundaries, i.e., oriented plate samples vs. unoriented tube samples. It appears that it is the microscopic ordering of the probe that is greatly affected, and it is conjectured that this is due to (a) strong cooperative lateral and interbilayer forces prevailing in the headgroup regions for the well-aligned samples and (b) a very distinctive requirement for packing the stearamide into the ordered array.

(4) Further studies with headgroup-labeled DPPC would be desirable to confirm and amplify these observations.

Acknowledgment. We acknowledge support for this research by NSF Grant No. DMR 77-17510 and NIH Grant No. GM 25862-02. E. M. is thankful for a Chaim Weizmann Fellowship (1977–9).

References and Notes

(1) E. Meirovitch and J. H. Freed, *J. Phys. Chem.*, previous paper in this issue.
(2) (a) L. Powers and N. A. Clark, *Proc. Natl. Acad. Sci. U.S.A.*, **72**, 840 (1975); (b) L. Powers and P. S. Pershan, *Biophys. J.*, **20**, 137 (1977); (c) L. Powers, Thesis, Harvard University, 1977.
(3) (a) B. J. Gaffney and H. M. McConnell, *J. Magn. Reson.*, **16**, 1 (1974); (b) J. F. Becker, J. Breton, N. E. Geacintov, and F. Trentacosti, *Biochim. Biophys. Acta*, **440**, 531 (1976); P. Mathis, J. Breton, A. Vermeglio, and M. Yates, *FEBS Lett.*, **63**, 171 (1976).
(4) (a) L. J. Berliner, Ed., "Spin Labeling—Theory and Applications", Academic Press, 1976. (b) S. Schreier, C. F. Polnaszek, and I. C. P. Smith, *Biochim. Biophys. Acta*, **515**, 375 (1978).
(5) J. B. Stomatoff, W. F. Graddick, L. Powers, and D. E. Moncton, *Biophys. J.*, **25**, 253 (1979).
(6) R. G. Griffin, L. Powers, and P. S. Pershan, *Biochemistry*, **17**, 2718 (1978).
(7) Z. Luz and S. Meiboom, *J. Chem. Phys.*, **59**, 275 (1973).
(8) E. Meirovitch, Z. Luz, and S. Alexander, *Phys. Rev. A*, **15**, 408 (1977); E. Meirovitch, Z. Luz, and S. Alexander, *Mol. Phys.*, **37**, 1489 (1979).
(9) (a) G. Moro and J. H. Freed, *J. Phys. Chem.*, **84**, 2837 (1980); (b) W. J. Lin and J. H. Freed, *J. Phys. Chem.*, **83**, 379 (1979).
(10) (a) G. Zaccai, G. Büldt, A. Seelig, and J. Seelig, *J. Mol. Biol.*, **134**, 693 (1979); (b) G. Büldt, H. V. Gally, J. Seelig, and G. Zaccai, *Ibid.*, **134**, 673 (1979); (c) G. Büldt, H. V. Gally, A. Seelig, and J. Seelig, *Nature (London)*, **271**, 182 (1978).
(11) R. G. Griffin, *J. Am. Chem. Soc.*, **98**, 851 (1976).
(12) R. F. Campbell, E. Meirovitch, and J. H. Freed, *J. Phys. Chem.*, **83**, 525 (1979).
(13) (a) J. S. Hwang, R. P. Mason, L. P. Hwang, and J. H. Freed, *J. Phys. Chem.*, **79**, 489 (1975); (b) C. F. Polnaszek and J. H. Freed, *Ibid.*, **79**, 2283 (1975).
(14) R. F. Campbell and M. W. Hanna, *J. Phys. Chem.*, **80**, 1892 (1976).
(15) (a) R. L. Humphries and G. R. Luckhurst, *J. Chem. Phys.*, **54**, 1491 (1971); (b) J. Pilar, J. Labsky, J. Kalal, and J. H. Freed, *J. Phys. Chem.*, **83**, 1907 (1979).
(16) R. P. Mason, C. F. Polnaszek, and J. H. Freed, *J. Phys. Chem.*, **78**, 1324 (1974).
(17) A. Keith and D. Chapman, *Biochemistry*, **16**, 634 (1977).
(18) S. A. Asher and P. S. Pershan, *J. Phys.*, **40**, 161 (1979).
(19) Y. Galerne, *J. Phys. Lett.*, **40**, L-73 (1979).
(20) (a) G. R. Luckhurst, M. Ptak, and A. Sanson, *J. Chem. Soc., Faraday Trans 2*, **69**, 1752 (1973); (b) E. Meirovitch and Z. Luz, *Mol. Phys.*, **30**, 1589 (1975).
(21) R. G. Griffin, private communication.